J Therm Anal Calorim (2011) 103:501–506
DOI 10.1007/s10973-010-0892-8

Synthesis and optical and structural characterization of $Ce_{(1-x)}O_2$:M_xO (M = Cu, Co) pigments

V. D. Araújo · M. I. B. Bernardi

Received: 19 April 2010 / Accepted: 14 May 2010 / Published online: 30 May 2010

Abstract The synthesis of pigments from the system $Ce_{1-x}O_2$–M_xO (M = Cu, Co) was achieved via a polymeric precursors method, Pechini method. Differential scanning calorimetry (DSC) and thermogravimetry (TG) techniques were used to accurately characterize the distinct thermal events occurring during synthesis. The TG and DSC results revealed a series of decomposition temperatures due to different exothermal events, which were identified as H_2O elimination, organic compounds degradation, and phase formation. X-Ray diffraction patterns show the presence of pure cubic CeO_2 phase for the samples with low Cu and Co loading. A decrease of the specific surface area with increasing copper and cobalt content was observed. The UV–visible diffuse reflectance technique was employed to study the optical properties in the 200–800 nm range. Colorimetric coordinates L^*, a^*, b^* were calculated for the pigment powders. The powders presented a variety of colors from yellow for pure CeO_2, to brown for the ones loaded with copper and gray for the ones with cobalt.

Keywords Pechini method · CeO_2 · Pigments · Copper · Cobalt

Introduction

Inorganic pigments have been utilized by mankind since ancient times, however, most of the inorganic pigments contain heavy metals such as Cd, Cr, Hg, Pb, and Se that can adversely affect the environment and human health when critical levels are exceeded. Therefore, development of safe inorganic pigments has been required in order to replace the toxic inorganic pigments with environment-friendly pigments or less toxic substances [1, 2]. Development of safe inorganic alternatives is essential, as the use of high-performance organic pigments have some limitations because of their thermal and ultraviolet (UV) ray radiation instabilities [3].

Ceria (CeO_2) has earned intensive interest in the past decade because it plays a vital role in emerging technologies for environmental and energy-related applications [4]. CeO_2 has found its applications in many aspects, such as fast-response gas sensors, ultraviolet ray detector, and gamma radiation dosimetry [5]. It can be used as an additive to glass (2–4%) to protect light-sensitive materials, as a coating for corrosion protection of metals, as an oxidation catalyst, and as a counter electrode for electrochromic devices [6].

A variety of studies demonstrated the use of CeO_2 as an alternative environment-friendly inorganic pigment [1–3, 7–10]. Various methods have been employed to synthesize CeO_2 particles such as coprecipitation [11–13], microemulsion [14], urea combustion method [15], sonochemical method under ambient air [6, 16], hydrothermal and microwave-assisted hydrothermal method [6, 17, 18], and via a sol–gel route [19].

This work involved the synthesis of $Ce_{1-x}O_2$–M_xO (M = Cu, Co) system, with $x = 0$, 0.03, 0.05, and 0.10 powders and a study of their thermal behavior as a function of the structural and optical properties for pigment applications. The samples were prepared by the polymeric precursor method. This method, also called the Pechini method [20], allows for the production of nanocrystalline

V. D. Araújo (✉) · M. I. B. Bernardi
Instituto de Física de São Carlos, USP – Universidade de São Paulo, Av. Trabalhador São-carlense, 400, Sao Carlos, SP 13560-970, Brazil
e-mail: dantas@ursa.ifsc.usp.br

powder samples at relatively low temperatures. This synthesis produces a polymer network starting from a polyhydroxy alcohol and an alpha-hydroxycarboxylic acid, with metallic cations homogeneously distributed throughout the matrix [21]. The samples were characterized by thermal analysis, thermogravimetric and differential scanning calorimetry, X-ray diffraction, BET specific surface area, diffuse reflectance, and colorimetric coordinate techniques.

Experimental procedure

The polymeric precursor method is based on the polymerization of metallic citrate using ethylene glycol. A hydrocarboxylic acid such as citric acid is normally used to chelate cations in an aqueous solution. The addition of a polyalcohol such as ethylene glycol leads to the formation of an organic ester. Polymerization promoted by heating to around 100 °C results a homogenous resin in which the metal ions are distributed uniformly throughout the organic matrix. The resin is then calcined to produce the desired oxides [22].

Cerium ammonium nitrate, $(NH_4)_2Ce(NO_3)_6$, copper nitrate, $Cu(NO_3)_2{\cdot}3H_2O$, and cobalt nitrate, $Co(NO_3)_2{\cdot}6H_2O$, were used as precursors. The cerium ammonium nitrate and copper nitrate were dissolved in water and then mixed into an aqueous citric acid solution (100 °C) under constant stirring. The pH of the solution was adjusted to 6 with ammonia. Next, ethylene glycol ($HOCH_2CH_2OH$) was added to polymerize the citrate by a polyesterification reaction. The citric acid:metal molar ratio was 3:1, while the citric acid:ethylene glycol mass ratio was 60:40. The compositions studied here are $Ce_{1-x}O_2{:}M_xO$ (M = Cu, Co), where x (%mol) = 0, 0.03, 0.05, and 0.10.

The thermal decomposition and crystallization processes were studied by TG (Netzsch STA 409C) and DSC techniques in an oxygen atmosphere at a heating rate of 10 °C min^{-1}. Al_2O_3 was used as reference material during the thermal analysis.

After annealing at 600 °C for 2 h, the powders were structurally characterized using an automatic X-ray diffractometer (Rigaku, Rotaflex RU200B) with CuKα radiation (50 kV, 100 mA, $\lambda = 1.5405$ Å) and in a θ–2θ configuration using a graphite monochromator. The scanning range was between 20° and 90° (2θ), with a step size of 0.02° and a step time of 5.0 s. The Rietveld analysis was performed with the Rietveld refinement program GSAS [23]. A pseudo-Voigt profile function was used. The specific surface area (BET) was estimated from the N_2 adsorption/desorption isotherms at liquid nitrogen temperature, using a Micrometrics ASAP 2000. Uv–visible diffuse reflectance spectra were acquired using a Cary 5G spectrophotometer in the 200–800 nm range. Colorimetric coordinates of the pigments were measured in the 400 and 700 nm range, using a spectrophotometer (Minolta, CM2600d) equipped with standard type D65 (day light) light source, following the CIE-$L^*a^*b^*$ colorimetric method recommended by the CIE (Commission Internationale de l'Eclairage) [24].

Results and discussion

It is well known that metal complexation and polymerization reactions occur during synthesis by the polymeric precursor method [22]. In the material studied here, the complexation of copper and cobalt with citric acid led to the following reactions:

$$Cu(NO_3)_2{\cdot}3H_2O + 2C_6O_7H_8 \rightarrow Cu(C_6O_7H_7)_2 + 2HNO_3 + 3H_2O \quad (1)$$

and

$$Co(NO_3)_2 \cdot 6H_2O + 2C_6O_7H_8 \rightarrow Co(C_6O_7H_7)_2 + 2HNO_3 + 6H_2O \quad (2)$$

forming nitric acid and water. The cerium complexation reaction occurred as follows:

$$(NH_4)_2Ce(NO_3)_6 + 6C_6O_7H_8 \rightarrow Ce(C_6O_7H_7)_6 + 2NH_4 + 6HNO_3 \quad (3)$$

with the formation of ammonium, nitric acid, and water.

Mixing these metallic complexes (metallic citrates) above 70 °C triggered the onset of the esterification reaction between metal citrate and ethylene glycol, as follows:

$$M^{n+}[OCOCH_2C(OH)(COOH)CH_2COOH]_x + 3HOCH_2CH_2OH \rightarrow M^{n+}\left[OCOCH_2C(OH)(COOH)CH_2COOCH_2CH_2OH\right]_x + x'H_2O \quad (4)$$

In the compounds studied here, the polyesterification reactions (Reaction 4) occurred continuously until the polymer network was formed. Therefore, the main organic compounds contained in the resin were alcohol, water, ammonium, nitric acid, and polyester.

Figure 1 presents the TG and DSC curves of the $Ce_{1-x}O_2{:}M_xO$ (M = Cu, Co) systems. Although the method is basically semi-quantitative, mass variations can be measured accurately. The TG curves revealed a series of overlapping decomposition reactions due to different exothermal events, which are indicated by the DSC curves.

The TG curves of all samples showed three events of mass loss: the first event (50–150 °C) was attributed to the elimination of the adsorbed water. The second (150–300 °C) and third (300–500 °C) events were attributed to the breakage of the organic chains and total thermal

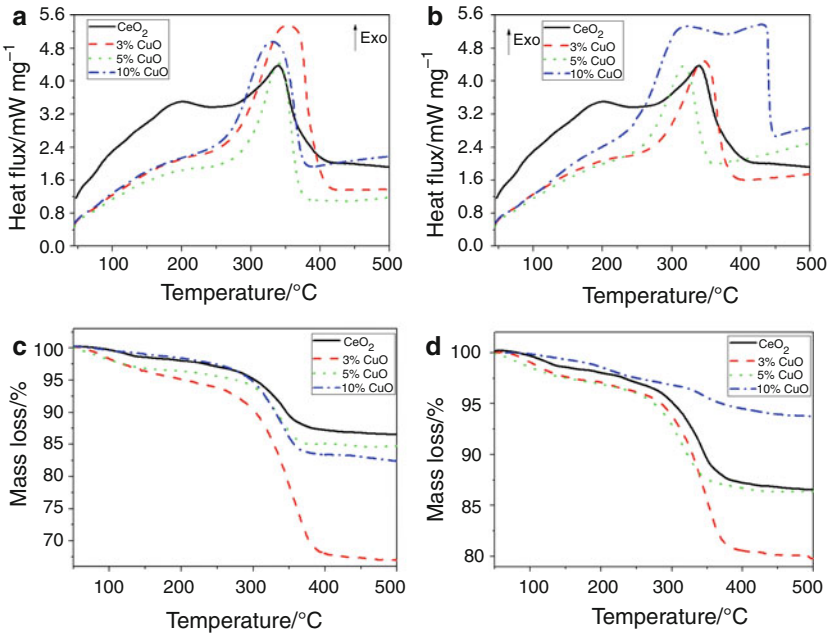

Fig. 1 **a** DSC curves of the $Ce_{1-x}O_2$:Cu_xO systems, **b** DSC curves of the $Ce_{1-x}O_2$:Co_xO systems, **c** TG curves of the $Ce_{1-x}O_2$:Cu_xO systems and **d** TG curves of the $Ce_{1-x}O_2$:Co_xO

degradation [25]. The DSC curves presented exothermal reactions during the oxidative thermal decomposition, due to several events of thermal decomposition of the organic material.

Figure 1a, b showed a shift towards higher temperatures of the exothermal peak centered around 250 and 400 °C for samples with 3% copper and cobalt content. In contrast, for samples with 5 and 10% Cu and Co this shift occurs for lower temperatures. This finding allows us to conclude that the inclusion of 5% or more of Cu and Co to the ceria lowers the phase formation temperature to obtain crystalline materials without organic compounds.

Figure 2 shows the XRD patterns for $Ce_{1-x}O_2$:M_xO samples. Fluorite type CeO_2 (ICSD no 156250) was present in all samples. Secondary phases were found only in sample with 10% Cu loading, and in samples with 5 and 10% Co loading. It should be noted that the precise state of copper and cobalt oxide in $Ce_{1-x}O_2$:M_xO (M = Cu, Co) catalysts is still debated in literature [26]. It has been proposed that the absence of secondary phases indicates that copper and cobalt species could be highly dispersed (bulk and/or surface) in ceria [15, 19, 26–34], or the formation of a solid solution with Cu^{2+} or Co^{2+} species substituting Ce^{4+} [15, 19, 26–28, 30, 31, 34].

Rietveld refinement showed an increase in lattice parameter *a*, presented in Table 1, with higher copper content, while a decrease in the lattice parameter occurs for the ones loaded with cobalt. Kumar et al. [34] observed a decrease in the lattice parameter *a* with increasing cobalt content. They attributed this behavior to substitution of bigger Ce^{4+} ion (radii 0.97 Å) by the smaller Co^{2+} ion

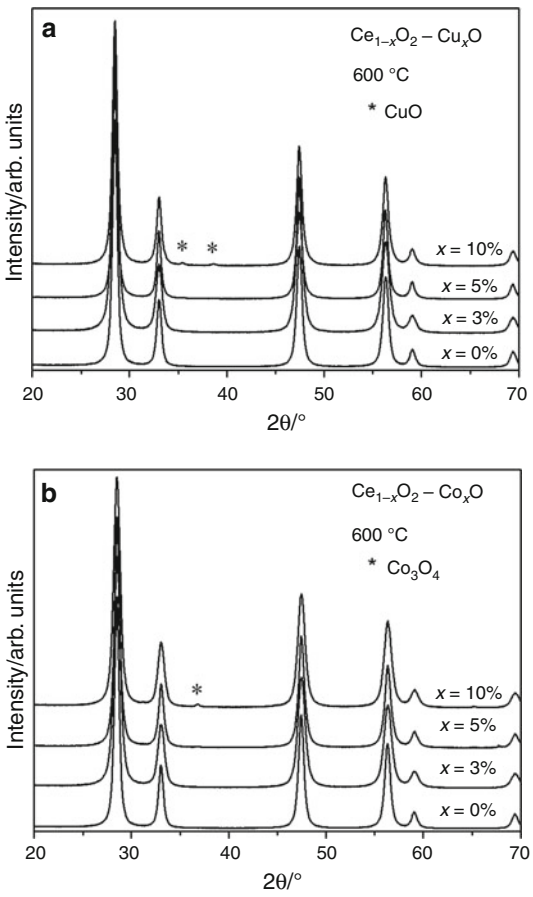

Fig. 2 X-ray diffraction patterns of: **a** $Ce_{1-x}O_2$:Cu_xO, and **b** $Ce_{1-x}O_2$:Co_xO systems, calcined at 600 °C/2 h

(radii 0.72 Å). We believe the same could be happening in our samples.

A first-principles density functional (DF) calculations performed by Wang et al. [35] showed that the Cu cations do not fit well in the standard positions for the Ce cations in the ceria lattice and tend to adopt a nearly planar, four-coordinated first shell. They also observed that the introduction of oxygen vacancies in the DF calculations did not lift the atypical coordination of Cu cations and led to small expansions in the cell dimensions.

Thus, the increase in the lattice parameter, *a*, of the samples loaded with copper is due to the insertion of Cu cations in the ceria matrix and the formation of oxygen vacancies for samples with 1, 3, and 5% Cu content, and also the formation of CuO phase for the sample with 10% Cu.

Table 1 presents the BET specific surface area, the density, and the equivalent spherical diameter of the samples. A non-linear behavior is observed for the specific surface area of the catalysts. For the samples with copper, first there is an increase in the surface area up to 3% copper content, followed by a decrease for the sample with 5% Cu and a subsequent increase for the sample with 10% copper content. For the ones with cobalt, first there is an increase in the surface area up to 3% cobalt content, followed by a decrease for the samples with 5 and 10% cobalt content. The equivalent spherical diameter of the samples presented an inverse behavior in comparison with the specific surface area.

Figure 3 presents the UV–visible spectra for the $Ce_{1-x}O_2$:M_xO samples. The shoulder around 350 nm becomes less intense with an increase in copper or cobalt content. For the samples loaded with copper, Fig. 3a, two characteristics bands are observed: one around 450 nm due to an emission and absorption of a photon by Cu^+ complexes and/or absorption from the conduction band of metallic copper and another between 600 and 800 nm corresponding to *d*–*d* transitions of Cu^{2+} in an octahedral O_h configuration more or less tetragonally distorted, the wavelength decreasing as the distortion increases [36]. For the samples containing cobalt, Fig. 3a, two bands are also observed: one around 430–450 nm due to the $^1A_{1g} \xrightarrow{\nu_2} {}^1T_{2g}$ transition of octahedral Co^{3+} species, and another around 730 nm due to the $^1A_{1g} \xrightarrow{\nu_1} {}^1T_{1g}$ transition of octahedral Co^{3+} species [37].

Table 2 presents the colorimetric coordinates (*L**, *a**, *b**) of $Ce_{1-x}O_2$:M_xO (M = Cu, Co) powder systems, using type D65-10° (day light) light source, according to the CIE-*L*a*b** standard colorimetric method. These colorimetric coordinates must be analyzed jointly to determine the final color of pigments, especially the *a** and *b** coordinates. The pure CeO_2 sample presented a light-yellow color. The samples become greenish with copper content and brownish with cobalt content.

Table 1 Lattice parameter (*a*), specific surface area, density and BET spherical diameter of the $Ce_{1-x}O_2$:M_xO (M = Cu,Co) samples

Sample	*a*/nm*	$A_s/m^2/g$	$\rho/g/cm^{3a}$	d_{BET}/nm
CeO_2	5.4164	40.4	7.16	21
CeO_2 3%Cu	5.4168	42.5	7.06	20
CeO_2 5%Cu	5.4184	30.6	6.99	28
CeO_2 10%Cu	5.4192	43.6	7.15	19
CeO_2 3%Co	5.4160	64.4	7.04	13
CeO_2 5%Co	5.4165	40.4	6.97	21
CeO_2 10%Co	5.4149	34.6	7.15	24

[a] Calculated from the Rietveld refinement

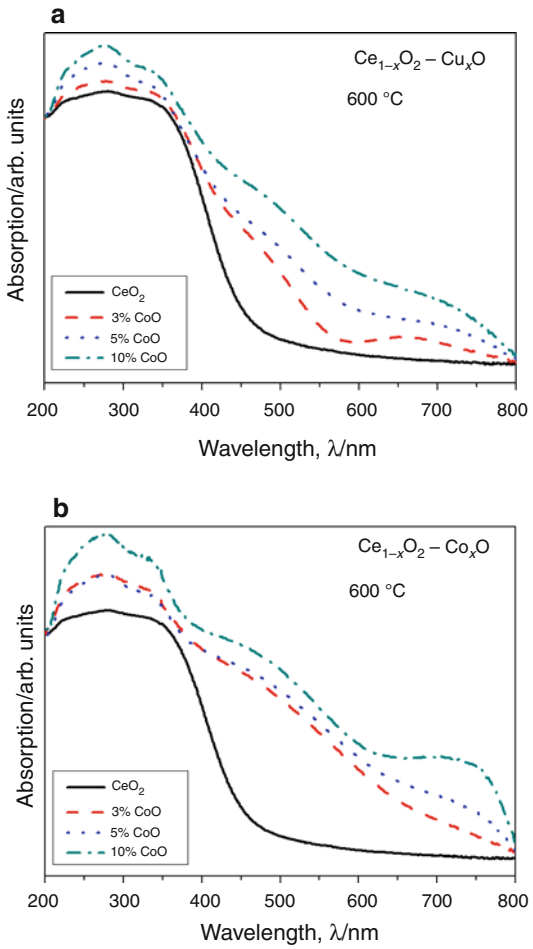

Fig. 3 UV–visible diffuse reflectance spectra of: **a** $Ce_{1-x}O_2$:Cu_xO, and **b** $Ce_{1-x}O_2$:Co_xO systems, calcined at 600 °C/2 h

Table 2 Colorimetric coordinates (L^*, a^*, and b^*) $Ce_{1-x}O_2$:M_xO (M = Cu,Co) powders systems, using light source type D65-10° (day light), following the CIE-$L^*a^*b^*$ standard colorimetric method

Sample	L^*	a^*	b^*
CeO_2	95.21	−1.48	10.64
CeO_2 3%Cu	75.99	1.03	20.42
CeO_2 5%Cu	67.22	2.63	13.90
CeO_2 10%Cu	59.25	3.27	12.20
CeO_2 3%Co	65.32	6.58	17.37
CeO_2 5%Co	56.11	5.19	13.15
CeO_2 10%Co	49.17	3.79	9.98

Conclusions

The polymeric precursor method proved efficient to synthesize pigments with colors ranging from yellow to brown and gray. Powders of the system $Ce_{1-x}O_2$:M_xO (M = Cu, Co) were synthesized as a single phase with the position of the X-ray diffraction plane showing a good match with the values indexed in crystallographic phase cards. The DSC and TG techniques allowed to determine the temperature range of processes: degradation of the polymer (pyrolysis of the organic compounds), elimination of nitrates, and water and phase formation. For the powders obtained the inclusion of 5% or more of Cu and Co to the ceria lowers the phase formation temperature to obtain crystalline materials without organic compounds. The specific surface area and the colorimetric coordinates were determined for all the samples.

Acknowledgements The authors are indebted to Prof. Elson Longo for the use of the BET facility. The authors also gratefully acknowledge the financial support of the Brazilian research funding agencies FAPESP, CAPES and CNPq.

References

1. Kumari LS, Rao PP, Reddy ML. Environment-friendly red pigments from CeO_2-Fe_2O_3-Pr_6O_{11} solid solution. J Alloys Compd. 2008;461:509–15. doi:10.1016/j.jallcom.2007.07.055.
2. Furukawa S, Masui T, Imanaka N. Synthesis of new environment-friendly yellow pigments. J Alloys Compd. 2006;418:255–8. doi:10.1016/j.jallcom.2005.08.108.
3. Sreeram KJ, Srinivasan R, Devi JM, Nair BU, Ramasami T. Cerium molybdenum oxides for environmentally benign pigments. Dyes Pigments. 2007;75:687–92. doi:10.1016/j.dyepig.2006.07.021.
4. Sun C, Sun J, Xiao G, Zhang H, Qiu X, Li H, Chen L. Mesoscale organization of nearly monodisperse flowerlike ceria microspheres. J Phys Chem B. 2006;110(27):13445–52. doi:10.1021/jp062179r.
5. Li Y, Dong X, Gao J, Hei D, Zhou X, Zhang H. A highly sensitive γ-radiation dosimeter based on the CeO_2 nanowires. Phys E. 2009. doi:10.1016/j.physe.2009.04.036.
6. Wang H, Zhu J-J, Zhu J-M, Liao X-H, Xu S, Ding T, Chen H-Y. Preparation of nanocrystalline ceria particles by sonochemical and microwave assisted heating methods. Phys Chem Chem Phys. 2002;4:3794–9. doi:10.1039/b201394k.
7. Llusar M, Vitásková L, Šulcová P, Tena MA, Badenes JA, Monrós G. Red ceramic pigments of terbium-doped ceria prepared through classical and non-conventional coprecipitation routes. J Eur Ceram Soc. 2010. doi:10.1016/j.jeurceramsoc.2009.08.005.
8. Šulcová P, Vitásková L, Trojan M. Thermal analysis of the $Ce_{1-x}Tb_xO_2$ pigments. J Therm Anal Calorim. 2010. doi:10.1007/s10973-009-0129-x.
9. Strnadlová L, Šulcová P, Llusar M. Thermal study of the $Ce_{0.9}Tb_{0.1}O_2$ pigment prepared by different synthesis. J Therm Anal Calorim. 2010. doi:10.1007/s10973-009-0644-9.
10. Santos SF, de Andrade MC, Sampaio JA, da Luz AB, Ogasawara T. Thermal study of TiO_2–CeO_2 yellow ceramic pigment obtained by the Pechini method. J Therm Anal Calorim. 2007;87:743–6. doi:10.1007/s10973-006-7754-4.
11. Avgouropoulos G, Ioannides T, Papadopoulou Ch, Batista J, Hocevar S, MAtralis HK. A comparative study of Pt/γ-Al_2O_3, Au/α-Fe_2O_3 and CuO–CeO_2 catalysts for the selective oxidation of carbon monoxide in excess hydrogen. Catal Today. 2002;75:157–67. doi:10.1016/S0920-5861(02)00058-5.
12. Gutiérrez-Ortiz JI, de Rivas B, López-Fonseca R, González-Velasco JR. Study of the temperature-programmed oxidative degradation of hydrocarbons over Ce-based catalysts by evolved gas analysis. J Therm Anal Calorim. 2007;87:55–60. doi:10.1007/s10973-006-7812-y.
13. Nasser H, Rédey A, Yuzhakova T, Kovács J. Thermal stability and surface structure of Mo/CeO_2 and Ce-doped Mo/Al_2O_3 catalysts. J Therm Anal Calorim. 2009;95:69–74. doi:10.1007/s10973-008-9050-y.
14. Babu S, Thanneeru R, Inerbaev T, Day R, Masunov AE, Schulte A, Seal S. Dopant-mediated oxygen vacancy tuning in ceria nanoparticles. Nanotechnology. 2009;20:085713. doi:10.1088/0957-4484/20/8/085713.
15. Delimaris D, Ioannides T. VOC oxidation over CuO–CeO_2 catalysts prepared by a combustion method. Appl Catal B. 2009;89:295–302. doi:10.1016/j.apcatb.2009.02.003.
16. Miao J-J, Wang H, Li Y-R, Zhu J-M, Zhu J-J. Ultrasonic-induced synthesis of CeO_2 nanotubes. J Cryst Growth. 2005;281:525–9. doi:10.1016/j.jcrysgro.2005.04.058.
17. Gao F, Lu Q, Komarneni S. Fast synthesis of cerium oxide nanoparticles and nanorods. J Nanosci Nanotechnol. 2006;6:3812–9. doi:10.1166/jnn.2006.609.
18. Han W-Q, Wu L, Zhu Y. Formation and oxidation state of CeO_{2-x} nanotubes. J Am Chem Soc. 2005;127:12814–5. doi:10.1021/ja054533p.
19. Chen J, Zhu J, Zhan Y, Lin X, Cai G, Wei K, Zheng Q. Characterization and catalytic performance of Cu/CeO_2 and Cu/MgO-CeO_2 catalysts for NO reduction by CO. Appl Catal A. 2009;36:208–15. doi:10.1016/j.apcata.2009.05.017.
20. Pechini M. Method of preparing lead and alkaline-earth titanates and niobates and coating method using the same to form a capacitor. US Patent 3 330 697. 1967.
21. Kakihana M. Invited review ''sol–gel'' preparation of high temperature superconducting oxides. J Sol–Gel Sci Technol. 1996;6:7–55. doi:10.1007/BF00402588.
22. Bernardi MIB, Araújo VD, Mesquita A, Frigo GJM, Maia LJQ. Thermal, structural and optical properties of Al_2CoO_4-crocoite composite nanoparticles used as pigments. J Therm Anal Calorim. 2009;97:923–8.
23. Larson AC, Von Dreele RB. Los Alamos National Laboratory. Los Alamos, EUA. Copyright. 1985–2000. The Regents of the University of California. 2001.
24. CIE. Recommendations of uniform color spaces, color difference equations, phychometrics color terms. Supplement no.2 of CIE

Publ. No. 15 (E1e1.31) 1971, Bureau Central de la CIE, Paris; 1978.
25. Xavier CS, Costa CEF, Crispim SCL, Bernardi MIB, Maurera MAMA, Conceição MM, Longo E, Souza AG. Synthesis of ZrO_2-based ceramic pigments. J Therm Anal Calorim. 2004;75:461–6. doi:10.1023/B:JTAN.0000027133.90639.1a.
26. Avgouropoulos G, Ioannides T, Matralis H. Influence of the preparation method on the performance of CuO-CeO_2 catalysts for the selective oxidation of CO. Appl Catal B. 2005;56:87–93. doi:10.1016/j.apcatb.2004.07.017.
27. Li Y, Fu Q, Flytzani-Stephanopoulos M. Low-temperature water-gas shift reaction over Cu- and Ni-loaded cerium oxide catalysts. Appl Catal B. 2000;27:179–91. doi:10.1016/S0926-3373(00)00147-8.
28. Bera P, Priolkar KR, Sarode PR, Hedge MS, Emura S, Kumashiro S, Lalla NP. Structural investigation of combustion synthesized Cu/CeO_2 catalysts by EXAFS and other physical techniques: formation of a $Ce_{1-x}Cu_xO_{2-\delta}$ solid solution. Chem Mater. 2002;14:3591–601. doi:10.1021/cm0201706.
29. Bera P, Aruna ST, Patil KC, Hedge MS. Studies on Cu/CeO_2: a new no reduction catalyst. J Catal. 1999;186:36–44. doi:10.1006/jcat.1999.2532.
30. Lamonier C, Bennani A, Dhuysser A, Aboukais A, Wrobel G. Evidence for different copper species in precursors of copper-cerium oxide catalysts for hydrogenation reactions—an X-ray diffraction, EPR and X-ray photoelectron spectroscopy study. J Chem Soc Faraday Trans. 1996;92:131–6. doi:10.1039/FT9969200131.
31. Li L, Zhan Y, Zheng Q, Zheng Y, Chen C, She Y, Lin X, Wei K. Water–gas shift reaction over CuO/CeO_2 catalysts: effect of the thermal stability and oxygen vacancies of CeO_2 supports previously prepared by different methods. Catal Lett. 2009;130:532–40. doi:10.1007/s10562-009-9904-3.
32. Avgouropoulus G, Ioannides T. Effect of synthesis parameters on catalytic properties of CuO-CeO_2. Appl Catal B. 2006;67:1–11. doi:10.1016/j.apcatb.2006.04.005.
33. Liu J, Zhao Z, Wang J, Xu C, Duan A, Jiang G, Yang Q. The highly active catalysts of nanometric CeO_2-supported cobalt oxides for soot combustion. Appl Catal B. 2008;84:185–95. doi:10.1016/j.apcatb.2008.03.017.
34. Kumar S, Kim YJ, Koo BH, Choi H, Lee CG. Structural and magnetic properties of Co doped CeO_2 nano-particles. IEEE Trans Magn. 2009;45:2439–41. doi:10.1109/tmag.2009.2018602.
35. Wang X, Rodriguez JA, Hanson JC, Gamarra D, Martinez-Arias A, Fernandez-Garcia M. Unusual physical and chemical properties of Cu in $Ce_{1-x}Cu_xO_2$ oxides. J Phys Chem B. 2005;109:19595–603. doi:10.1021/jp051970h.
36. Praliaud H, Mikhailenko S, Chajar Z, Primet M. Surface and bulk properties of Cu-ZSM-5 and Cu/Al_2O_3 solids during redox treatments. Correlation with the selective reduction of nitric oxide by hydrocarbons. Appl Catal B. 1998;16:359–74. doi:10.1016/S0926-3373(97)00093-3.
37. Brik Y, Kacimi M, Ziyad M, Bozon-Verduraz F. Titania-supported cobalt and cobalt-phosphorus catalysts: characterization and performances in ethane oxidative dehydrogenation. J Catal. 2001;202:118–28. doi:10.1006/jcat.2001.3262.